# Journal of Materials Chemistry B

Accepted Manuscript






ROYAL SOCIETY OF CHEMISTRY

www.rsc.org/materialsB

# Highly Bright Water-Soluble Silica Coated Quantum Dots with Excellent Stability

**Yunfei Ma, Yan Li, Shijian Ma, and Xinhua Zhong***

*Shanghai Key Laboratory of Functional Materials Chemistry, Institute of Applied Chemistry, East China University of Science and Technology, Shanghai 200237, China.*

Email: zhongxh@ecust.edu.cn; Fax: +86 21 6425 0281

## Abstract

Silica coating *via* Stöber method is an effective route to render luminescent quantum dots (QDs) with great biocompatibility, low toxicity and water-solubility for bioapplications. However, the bottleneck in this route is the access of highly luminescent, colloidally stable QD dispersion in alcoholic solution. Herein, we report a facile route based on Stöber method for the synthesis of isolated silica coated QDs (QD@$SiO_2$) with high emission efficiencies, tunable small size (less than 30 nm) and excellent stability. Prior to silica coating, the initial oil-soluble QDs were made dispersible in alcohol/water media by replacing the native hydrophobic ligands with adenosine 5'-monophosphate (AMP). Then, 3-mercaptopropyl-trimethoxysilane (MPS) was introduced to serve as silane nucleation primers. Finally, silica shell with controllable thickness was obtained on QD surface by hydrolysis/condensation of tetraethyl orthosilicate (TEOS). Remarkably, the resultant QD@$SiO_2$ remain nearly the same high luminescent efficiency (50–65%) as that of initial oil-soluble QDs and exhibit excellent long-term photo and colloidal stability in harsh environments (pH range of 3–13, saturated NaCl solution and thermal treatment at 100 $^oC$). It was demonstrated that the cytotoxicity of the resultant QD@$SiO_2$ was significantly diminished. Moreover, the QD@$SiO_2$ conjugated with folic acid manifests high specific binding toward receptor-positive Hela cells over receptor-negative A549 cells, indicating the potential of our obtained QD@$SiO_2$ as robust biomarkers in cells due to their chemical processibility and low cytotoxicity.

## 1. Introduction

Colloidal luminescent quantum dots (QDs) are attracting increasing interest because of their novel size-dependent optoelectronic properties and excellent solution processibility, which make them have numerous potential applications in various fields including optoelectronics, photovoltaic cells, catalysis, and biomedicine.[1–7] One of the most promising applications of QDs is serving as an alternative fluorophore for fluorescence-based bioapplications ranging from medical diagnostics and tagging subcellular structure *in vitro* to luminescence imaging *in vivo*.[8–12] The premise behind this promising application is the access of high-quality water-soluble QDs (such as high emission efficiency, high photo and colloidal stability, and small particle size), which has been playing a critical role in this very active field. Typically, high-quality luminescent QDs are prepared via organic phase high-temperature route and the resultant QDs cannot disperse in aqueous media.[13–17] Obviously, this defect hinders their bioapplications to a great extent. In addition, there are many challenges that need to be addressed for the practical bioapplications of QDs, including photo and colloidal instability in harsh environments, and cytotoxicity caused by the heavy metal ions in QDs.[18–20]

In recent years, many strategies, such as ligand-exchange process,[9,21–24] cross-linking of QDs with amphiphilic polymers,[25–28] and silica coating,[8,29–33] have been made toward the fabrication of water-soluble QDs from the initial hydrophobic ones. Among them, silica coating is a very promising route because silica shell possesses excellent stability, nontoxicity, biocompatibility, and facile conjugation with various functional groups to enable the coupling and labeling of bio-targets with selectivity and specificity.[34–38] Up to now, silica coated QDs (QD@$SiO_2$) have generally been accomplished by the reverse microemulsion method.[39–48] This method can present an excellent ability in controlling the morphology of the resultant QD@$SiO_2$ with rather uniform sizes and good monodispersity. Unfortunately, the size (usually 30–150 nm) of the obtained QD@$SiO_2$ by this method is considered to be too bulky for subcellular labeling.[45] Meanwhile, the photoluminescence (PL) efficiency of the resultant QD@$SiO_2$ is quenched remarkably compared to that of the original ones,[30,39–41,46–48] even though some efforts have been made to improve the PL efficiency.[43,44]

Stöber method is an alternative approach to silica coating, which is based on sol-gel chemistry for growing spherical silica nanoparticles proposed by Stöber and co-workers in 1960s,[49] and then been further developed for silica growth around QDs in alcohol/water media.[29,50–55] This method can yield single or multiple QDs per silica sphere with controllable silica shell thickness ranging from a few to hundreds of nanometers. Thus, this method is promising in the access of small-sized QD@$SiO_2$ to be used in subcellular labeling. However, it should be noted that the prerequisite in this route is the access of alcohol-dispersible QDs with high PL brightness.[50] Conventionally, 3-mercaptopropyl-trimethoxysilane (MPS),[8,29,50] or 3-aminopropyl-trimethoxysilane (APS)[51] is used as the phase transfer reagents to make the initial oil-soluble QDs alcohol-soluble and further provide nucleation sites for the following silica coating. Nevertheless, the phase transfer process quenches the PL brightness remarkably and consequently results in QD@$SiO_2$ with poor emission efficiency. Therefore, the selection of suitable phase transfer reagents to obtain highly bright alcohol-soluble QDs is crucial for silica coating *via* Stöber method.

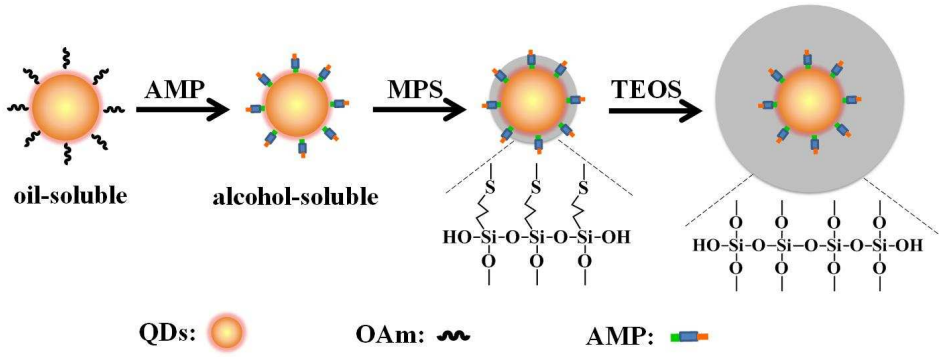


**Fig. 1** Schematic illustration for the synthesis of QD@$SiO_2$

Recently, a novel phase transfer reagent (adenosine 5'-monophosphate, AMP) has been proposed by our group,[56] and the resultant AMP-QDs can disperse homogeneously in alcohol media and retain high emission efficiency. We think the access of AMP-QDs paves a promising way to high-quality QD@$SiO_2$ *via* the Stöber method. Herein, we present a facile route to high-quality QD@$SiO_2$ (high emission efficiency, high photo and colloidal stability) *via* Stöber method starting from AMP-QDs. Firstly, highly luminescent oil-soluble QDs were prepared *via* the conventional organic phase high-temperature approach. Next, the oil-soluble

QDs were made alcohol-soluble by replacing the native hydrophobic ligands with AMP and MPS serving as silica nucleation primer was introduced. Finally silica shell with controllable thickness was obtained by hydrolysis of tetraethyl orthosilicate (TEOS) (Fig. 1). The resultant QD@$SiO_2$ exhibits high PL efficiencies (50–65%) and controllable particle size (< 30 nm in diameter). Furthermore, the resultant QD@$SiO_2$ shows extraordinary photo and chemical stability over extended periods of time in a broad pH range (3–13), even under saturated salt concentration (up to 4M NaCl solution) and thermal treatment at 100 $^{o}$C. Meanwhile, the silica shell could efficiently eliminate QD cytotoxicity of and provide a versatile bioconjugation. We expect that our obtained QD@$SiO_2$ with such superior features would be promising fluorophores for various bioapplications.

## 2. Experimental

### 2.1 Chemicals

Adenosine 5'-monophosphate (AMP), tetramethylammonium hydroxide pentahydrate (TMAH, >95%), oleylamine (OAm, 70%), 1-hexadecylamine (98%), 1-dodecylamine (>99%), oleic acid (99%), 1-octadecene (ODE, >95%), 3-mercaptopropyl-trimethoxysilane (MPS), aminopropyltriethoxysilane (APTES), folic acid (FA), N-Hydroxysuccinimide (NHS), dicyclohexylcarbodiimide (DCC), 3-(4,5-dimethylthiazol-2yl)-2,5-diphenyltetrazoliumbromide (MTT), sodium dodecyl sulfate (SDS) and 4',6-diamidino-2-phenylindole dihydrochloride (DAPI) were obtained from Aldrich and used without further purification. Tetraethylorthosilicate (TEOS), $NH_3 \cdot H_2O$ (25–28%), and dimethyl sulphoxide (DMSO) were ordered from Shanghai Lingfeng Chemical Reagent Co Ltd. DMEM (Dulbecco's modified Eagle's medium) supplemented with 10% fetal bovine serum was purchased from Shanghai Futurebio Technologies Co Ltd. All organic solvents including hexane, dichloromethane, ethanol and methanol were of analytical grade and obtained from commercial sources and used as received. Deionized (DI) water was used throughout.

### 2.2 Preparation of AMP-QDs *via* ligand exchange

The oil-soluble CdSe/CdS/ZnS QDs were first synthesized and the detailed procedure was available in the Electronic Supplementary Information (ESI). The ligand exchange was briefly performed as follows: 0.1 g of AMP was dissolved in 0.3 mL of ethanol and the pH value was adjusted to 10 with TMAH. The obtained AMP ethanol solution was added dropwise into a purified QDs solution in hexane ($10^{-6}$ M, 20.0 mL) and stirred for 30 min, and water was subsequently added. The colorless organic phase was discarded and the aqueous phase containing the QDs was collected and undergone centrifugation purification with use of acetone.

### 2.3 Coating AMP-QDs with silica shell

The QD@$SiO_2$ was prepared by a typical Stöber method as follows: AMP-QDs aqueous solution (2.0 mL with absorbance of 0.12 at the first absorption peak position, ~$1.2\times10^{-3}$ nmol QDs) was mixed with anhydrous alcohol (8.0 mL) in a 50 mL plastic centrifuge tube, followed by addition of MPS ethanol solution (35.0 μL, 1:100 by volume). The resultant reaction mixture was under vigorous shaking for 6 h in a shaker. Then a certain amount (0–20 μL) of TEOS and ammonia (100 μL) were added dropwise into the above mixture in turn. The reaction system was kept shaking for 16 h at room temperature for the overgrowth of silica shell around QDs. Finally, ethyl acetate was added to precipitate the formed QD@$SiO_2$ particles and terminate the silica coating reaction accordingly. The resultant QD@$SiO_2$ was purified by washing with ethanol and water in sequence and collected *via* centrifugation.

### 2.4 Conjugation of amino-functionalized QD@$SiO_2$ with folic acid

The amino groups were first grafted onto the surface of QD@$SiO_2$ for further bioconjugation with FA. Briefly, APTES ethanol solution (50.0 μL, 1:100 by volume) was added into crude QD@$SiO_2$ reaction solution and shaken for another 2 h in the dark condition. Then the resultant amine-functionalized QD@$SiO_2$ was collected *via* centrifugation and purified by washing with $H_2O$. The final APTES grafted QD@$SiO_2$ pellet was dispersed in DMSO (2.0 mL). FA (22.0 mg) was activated by DCC/NHS catalyst system (molar ratio of FA: DCC: NHS = 1:2:2) in anhydrous DMSO (2.0 mL) under stirring in the dark for 12 h at room

temperature. Then, activated FA (100 μL) was added dropwise into the APTES grafted QD@$SiO_2$ solution in DMSO to conduct the carboxy-amine coupling reaction and conjugation with the folic acid molecule. With shaking overnight, the resultant QD@$SiO_2$-FA samples were obtained through centrifugation (15000 r/min, 30min) and washed with $H_2O$ and finally re-dispersed in water.

**2.5 Cytotoxicity assay by MTT method**

Cytotoxicity was evaluated by performing MTT assays in the Hela cells. Cells were seeded at $5\times10^4$ per cell into a 96-well cell culture plate in DMEM with 10% fetal bovine serum at 37 °C and with 5% $CO_2$ for 24 h. Next, the cells were incubated with different concentrations of AMP-QDs and QD@$SiO_2$ for 24 h. After that time, MTT (10.0 μL, 5 mg/mL) was added to each well, and the plate was incubated for another 4 h at 37 °C. Cells were lysed with acidulated sodium dodecyl sulfate. Absorbance was measured at 570 nm using an automatic ELISA analyzer. Each data point was collected by averaging 6 samples in parallel and the blank cells were used as control.

**2.6 Cell labeling and fluorescent imaging**

To study the uptake and imaging of QD@$SiO_2$ -FA, Hela and A549 cells were cultured on glass chamber slides in a 6-well plate with 2.0 mL of DMEM medium with 10% (v/v) calf serum at 37 °C (5% $CO_2$), respectively. After 24 h of incubation, the cells were carefully rinsed with PBS (0.01 mol /L, pH 7.4), and the corresponding fresh media (2 mL) was added to the plates. Finally, QD@$SiO_2$-FA (20.0 μL) was added and mixed properly. Plates were returned to the incubator (37 °C, 5% $CO_2$) for 1 h. Then removing from culture medium, cells were fixed with 2% paraformaldehyde, washed with PBS, followed by DAPI staining (18.7 μM) of the nuclear for 5 min, washed with PBS for three times, and finally immersed in 30% (v/v) glycerol/PBS. Fluorescence images were recorded with 450–550/405 nm and 550–650/488 nm emission/excitation for the visualization of DAPI and QDs respectively.

**2.7 Characterization**

UV-vis and PL spectra were obtained on a Shimadzu UV-2450 UV-vis spectrophotometer and Cary Eclipse (Varian) fluorescence spectrophotometer, respectively. The PL QYs of QDs were calculated by the integrated emission of the QD samples in solution compared with that

of rhodamine 6G (PL QYs, 95%) in ethanol under identical optical density.[15] Transmission electron microscopy (TEM) images were taken on a JEOL JEM-1400 at an acceleration voltage of 100 kV. FT-IR spectra were measured with samples pressed into a KBr plate and recorded from 4000 to 400 $cm^{-1}$ using a Nicolet Magna-IR 550 FT-IR spectrometer. The absorbance at 570 nm in MTT assays was detected with spectrophotometric microplate reader (BioRad Model 550). Confocal fluorescence imaging was performed with an OLYMPUS ZX81 laser scanning microscopy and a 60× oil-immersion objective lens.

## 3. Results and disscussion

### 3.1 Silica coating of AMP-QDs

The initial oleylamine (OAm) capped oil-soluble CdSe/CdS/ZnS QDs were synthesized following standard literature method,[57–59] and the detailed procedure was available in the Electronic Supplementary Information (ESI). Exchange of the native hydrophobic ligands on oil-soluble QDs surface by AMP was performed according to our reported method.[56] AMP-QDs were selected for silica coating due to its high emission efficiency and excellent dispersibility in alcohol/water media,[56] which paves the way for the following hydrolysis/condensation of TEOS to grow silica shell on QD surface by the Stöber method. Notably, the access of alcohol-dispersible QDs with high brightness is difficult,[60,61] and becomes the main obstacle in the Stöber method. As expected, our obtained AMP-QDs show almost identical emission efficiency (50–65%) to that of the original oil-soluble one. To provide the nucleation site for TEOS condensation, MPS was then introduced to the AMP-QDs system. The terminal -SH group in MPS molecules can bind strongly to QD surface, leaving the silane group on the other end, from where the hydrolysis occurs and builds up a first thin silica shell to permit the following attachment of TEOS molecules. Homogeneous QD@$SiO_2$ with high PL efficiency and controllable shell thickness was successfully prepared *via* the following hydrolysis/condensation of TEOS. It should be noted that the silica coating process was conducted in plastic centrifuge tubes under shaking in a shaker at room temperature. This makes the fabrication process more reproducible and productive than the commonly adopted magnetic stirring methods.[34]

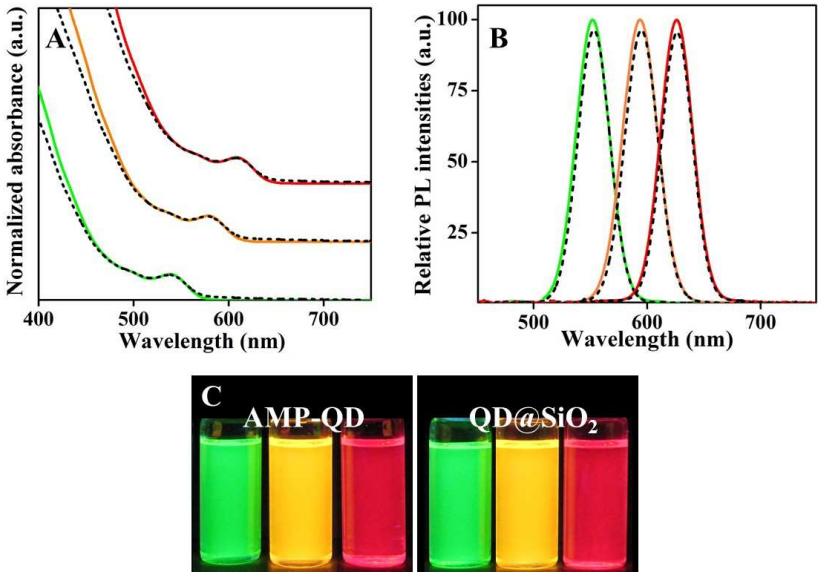


**Fig. 2** (A) UV-vis and (B) PL emission ($\lambda_{ex}$ = 400 nm) spectra of AMP-QDs aqueous solutions (solid curves), and the derivative QD@$SiO_2$ aqueous solutions (dashed curves). (C) luminescence images of AMP-QDs (left) and the derivative QD@$SiO_2$ (right) aqueous solutions under UV light irradiation. Note: the PL intensities of all AMP-QDs were normalized to 100, and the PL spectra of the derivative QD@$SiO_2$ were recorded under the same condition.

The silica coating experiments were performed on AMP-QDs with three typical emission wavelengths of 551, 592, and 625 nm (termed as $QD_{551}$, $QD_{592}$, $QD_{625}$, respectively hereafter). As shown in Fig. 2A,B, the derivative QD@$SiO_2$ aqueous solutions exhibited almost identical UV-vis absorption and PL emission spectral profiles to those of the original AMP-QDs. These results indicate that the process of silica coating has no effects on the electronic properties of the inorganic QD cores, and the obtained QD@$SiO_2$ maintain great dispersibility without obvious aggregation of the QDs inside the silica spheres. Notably, all the three studied QD@$SiO_2$ with different emission colors exhibit high PL efficiency of 50–65%, which are nearly the same values as those of AMP-QDs and the initial oil-soluble QDs. This was rarely observed in previous reports,[39–41,46–48,50–54] wherein a heavy loss of luminescence brightness of QDs after silica coating was obtained and thus hampering the practical application of QD@$SiO_2$ in luminescence imaging. The high emission efficiency of the obtained QD@$SiO_2$ was also demonstrated by the bright color images under UV lamp illumination (Fig. 2C).

There was almost no distinguishable luminescence brightness of the QDs before and after silica coating, which can be attributed to the fact that excellent photo and colloidal stability of AMP-QDs prevents the influence of hydrolysis of TEOS on the surface of QDs.

To reveal the silica coating, Fourier transform infrared (FT-IR) spectra of the initial oil-soluble OAm-capped QDs (simplified as OAm-QDs hereafter), AMP-QDs and QD@$SiO_2$ were measured. As can be seen from Fig. 3, the strong characteristic C-H stretching vibrations at 2800–3000 $cm^{-1}$ in OAm-QDs, derived from long hydrocarbon chain portion in OAm, almost disappeared in AMP-QDs, indicating that most OAm molecules originally attached on the QDs surface were replaced after phase transfer. Still weak vibrations at the same location can be observed maybe due to the small portion of hydrocarbon chain in AMP molecules. Simultaneously, the vibration of phosphate group (*ca.* 950–1100 $cm^{-1}$) and the purine ring (*ca.* 1450–1650 $cm^{-1}$) of the nucleotide in AMP-QDs appeared, confirming that the initial OAm capping molecules were indeed replaced by AMP in the process of phase transfer. With regard to the IR spectra of AMP-QDs and QD@$SiO_2$, both showed a broad band centered around 3500 $cm^{-1}$, corresponding to the O-H stretching bands of hydrogen-bonded water molecules (H-O-H) for the hydrophilic nature for both samples. For QD@$SiO_2$, the broad band could also be attributed to the SiO-H stretching of surface silanol hydrogen. The prominent difference of two spectra was the intense silicon-oxygen covalent bond vibrations appear mainly at 1110 $cm^{-1}$: there was a strong peak at 1110 $cm^{-1}$ for QD@$SiO_2$, while no apparent peak appeared for AMP-QDs. These results reveal the existence of a dense silica network, where oxygen atoms play the role of bridges between two silicon sites in QD@$SiO_2$. Furthermore, for QD@$SiO_2$, the symmetric stretching vibrations of Si-O-Si appear at 800 $cm^{-1}$, while its bending mode appears at 480 $cm^{-1}$. Also, the peak at 960 $cm^{-1}$ is assigned to the Si-OH on the surface, and the low energy band at 578 $cm^{-1}$ is assigned to Si-O stretching of the $SiO_2$ network defects for QD@$SiO_2$.[62,63] The FTIR spectroscopy analysis confirms that the siloxane group was introduced on the QD surface after silica coating.

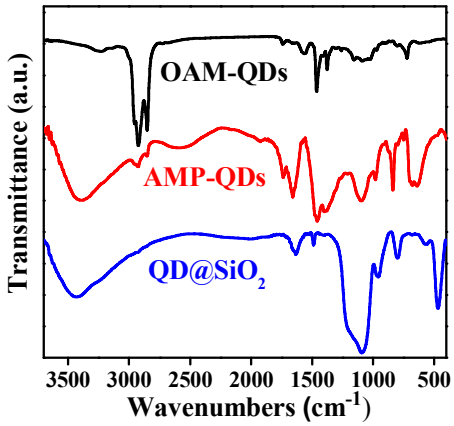


**Fig. 3** FTIR spectra of OAm-QDs, AMP-QDs and corresponding QD@$SiO_2$.

### 3.2 The effect of MPS and TEOS feeding concentration

To homogeneously encapsulate QDs in silica shell, it's generally required to find suitable silane primers prior to silica coating. Such a coupling agent can render QD surface vitreophilic and provide nucleation sites for depositing a silica shell on QD surface. In this study, MPS was chosen, since it contains a strong binding of the -SH groups to QD surface metal atoms, and leaves the silane groups on the other end, from where the hydrolysis occurs and builds up a first thin silica shell. Then TEOS began to hydrolyze on the basis of the first thin silica shell to form the outer thick shell. It was found that if MPS was not introduced into the solution, the hydrolysis of TEOS tended to form silica network in the alcohol/water media, but not a silica shell on the surface of QDs. Thus, MPS, as a surface primer, plays an important role for inducing the nucleation and growth of silica molecules around the QD and results in formation of isolated QD@$SiO_2$ particles. It should be noted that during the silica coating of QDs by Stöber method, MPS is usually used as both the phase transfer reagents for rendering the initial oil-soluble QDs alcohol-soluble and the nucleation sites for the following silica coating. The phase transfer process commonly quenches the PL brightness and consequently results in QD@$SiO_2$ with poor emission efficiency. Whereas, in this study, MPS was just used as a surface silane primer, and the phase transfer process was conducted with AMP, which could retain the high quality of initial oil-soluble QDs to give QD@$SiO_2$ with high luminescent efficiency.[56] It is mainly ascribed to the intrinsic molecular structure of

AMP with multiple functional groups that can chelate metal cations and potentially passivate QDs surface. Since the multidentate coordination mode of this ligand are weaker than covalent bonds, the surface ligands have no effects on the electronic properties of the inorganic QDs cores and therefore can preserve the quantum efficiency of the initial oil-soluble QDs.

After the surface attachment with MPS, there are three primary variables determining the following silica coating process, including $H_2O$/EtOH ratio, ammonia concentration, and amount of TEOS. The $H_2O$/EtOH solvent ratio affects the hydrolysis of TEOS, and a lower water content favors the nucleation and growth of silica around QD seeds. The adopted volume ratio was usually in the range of 1:1 to 1:5 in previous studies.[34, 52, 64] In this study, the $H_2O$/EtOH volume ratio was optimized to 1:4. Ammonia is known as a catalyst for TEOS hydrolysis and determining the hydrolysis rate. Isolated silica encapsulated QD sphere can be obtained only at suitable amount of ammonia with appropriate TEOS hydrolysis rate. The optimum amount of ammonia under our adopted experimental conditions is 100 μL. Irrespective of the composition of the EtOH/$H_2O$/$NH_3$ mixture, the amount of the added TEOS was found to play a critical role in determining the silica shell thickness of the resultant QD@$SiO_2$. In the following section, we will particularly discuss the effect of TEOS on the thickness of silica shell and the PL properties when the other experimental parameters were fixed.

To investigate the effect of different amounts of TEOS on the thickness of silica shell, the TEM images of oil-soluble $QD_{592}$ and the corresponding $QD_{592}$@$SiO_2$ prepared under different amounts of TEOS were measured and shown in Fig. 4. It was found that the size of the native $QD_{592}$ is 6.0±0.4 nm, while the derivative QD@$SiO_2$ spheres with mean diameter of 21±2.8 nm and 30±3.5 nm corresponding to silica thickness of ~8 and 12 nm were obtained under TEOS amount of 10 μL and 20 μL, respectively. Therefore, the expected silica size can be easily adjusted by varying the amount of TEOS used. Notably, single QD was encapsulated into a silica sphere to form the isolated QD@$SiO_2$ particle in most cases. In our statistic of over 200 nanoparticles, single QD per silica particle accounts for ~75% in the 21 nm sized QD@$SiO_2$, while in the 30 nm sized QD@$SiO_2$, this fraction is ~60%. A narrow size

distribution of the resultant QD@$SiO_2$ was also obtained, as shown in Fig. 4B,C. As we know, a coated single QD can maintain its spectra purity.[50] However, the target of silica particles containing single QD with uniform sizes is very difficult to be obtained via the Stöber route and therefore few successful samples were reported up to now.[50] In comparison, the above target can be more feasibly achieved via the reverse microemulsion strategies. Regretfully, the dimensions of the obtained QD@$SiO_2$ (in the range of 30–150 nm) by this route is considered to be too bulky for efficient labeling due to the subcellular features.[45] In our study, the obtained QD@$SiO_2$ not only contain single QD in silica particles but also showed smaller size and high PL efficiency, which makes them attractive in practical application in bio-imaging.

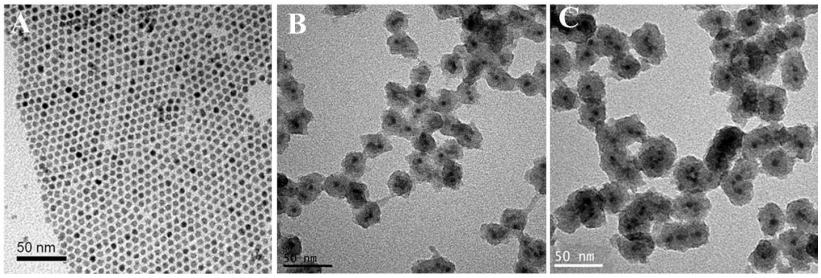


**Fig. 4** TEM images of (A) native oil-soluble QDs and corresponding QD@$SiO_2$ with use of (B) 10 μL, and (C) 20 μL of TEOS.

Furthermore, the dependence of PL efficiency of obtained QD@$SiO_2$ on the amount of TEOS used (i.e. the silica shell thickness) was also monitored and corresponding PL spectra were available in Fig. S1. The PL efficiency (62%) of the hydrophilic AMP-$QD_{592}$ was nearly identical to that of initial oil-soluble ones. The PL intensities of the AMP-QDs were almost completely preserved after silica coating with the addition of 10 μL TEOS. With the increase of TEOS amount to 20 μL, 86% of PL brightness of the AMP-QDs was still retained. It can be concluded that the thickness of silica shell has only slight effect on the PL efficiency of the resultant QD@$SiO_2$. The reason for this promising feature is definitely ascribed to the excellent stability of AMP-QDs to prevent the influence of hydrolysis of TEOS on the surface of QDs. It should be noted that huge drops of PL efficiency is always encountered during the silica coating process regardless of Stöber or reverse microemulsion route adopted.

### 3.3 Excellent photo and colloidal stability

The photo and colloidal stability in harsh environments is the premise of QDs biological applications. The formation of silica shell was expected to build great protection for the QDs core and offer excellent stability, while in most previous reports, the investigations were mainly focused on the preparation and few were devoted to the detailed investigation on their stability. In the following section, we will particularly discuss the pH sensitivity, electrolyte solution stability, photooxidation and thermal stability of our obtained QD@$SiO_2$.

**3.3.1 pH sensitivity.** Colloidal stability by the environmental pH is a critically important property of hydrophilic nanocrystalline materials. It is well-known that for biological applications, QDs are expected to be stable at least in pH 4–8 range.[65] To investigate the pH stability of the obtained QD@$SiO_2$, 100 μL of purified $QD_{592}$@$SiO_2$ was mixed with 4.9 mL of PBS buffer solution with different pH values (2–13) and then sealed and stored in the dark for the further investigation. The temporal evolution of relative PL intensities of QD@$SiO_2$ in different pH media was presented in Fig. 5A. As expected, the obtained QD@$SiO_2$ could maintain high PL efficiency and colloidal stability over months in a broad pH range (3–13). In the pH range of 3–13, high PL brightness could be preserved without obvious loss (< 5%), and there was no obvious aggregation of QDs within a time period of one month. In the extremely low pH of 2, the PL intensity decreased obviously with extending time, and dropped to 68% of the initial value after been stored for 30 days. Meanwhile, the aggregation of QD@$SiO_2$ also occurred gradually under this pH condition. Interestingly, the relative PL intensities have a 5–10% increase when the QDs dispersed in PBS buffer with pH of 7 to 13. This may be due to the light irradiation and/or air oxidization effect during the storage stage.

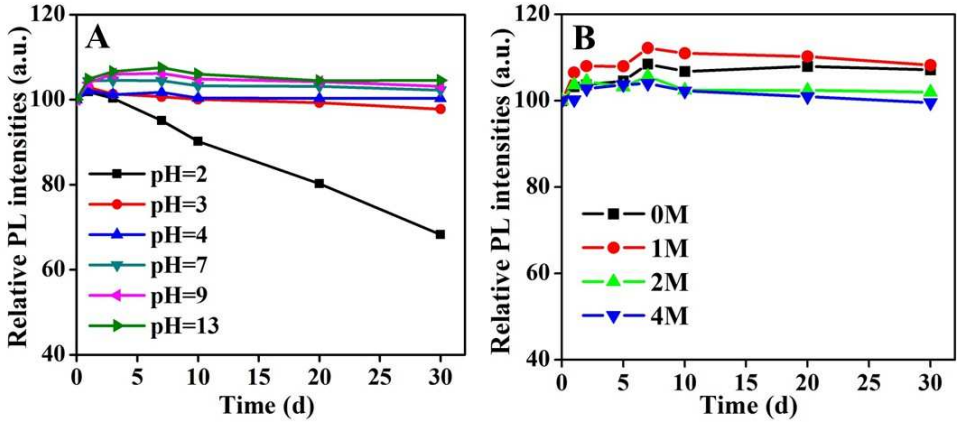

**Fig. 5** (A) Temporal evolution of relative PL intensities of QD@$SiO_2$ samples under different pH values. (B) Temporal evolution of relative PL intensities of QD@$SiO_2$ in NaCl solutions with different concentrations.

**3.3.2 Stability in electrolyte solution.** For the practical application in biological systems, such as intracellular and in vivo media where the ionic concentration is known to be high, QDs need to sustain long-term stability in a wide range of electrolyte concentrations. To test the colloidal stability of QD@$SiO_2$ in electrolyte solutions, the purified $QD_{592}$@$SiO_2$ solution were mixed with NaCl solution with concentration ranging from 0 to 4.0 M. Fig. 5B shows the temporal evolution of relative PL intensities of the QD@$SiO_2$ dispersed in different NaCl concentration solutions in a period of a month. The instant PL spectra of QD@$SiO_2$ dispersed in NaCl solutions of different concentrations kept a similar profile but with slightly variation in PL intensities. During the test period (30 days), the PL intensity of all samples dispersed in different concentration NaCl solutions did not show any reduction, but increased in a little bit (within 15%) as observed in the case of different pH media. The silica network provided AMP-QDs a stable hydration layer, which was little affected by charged ions. This may give the reason for the superficial colloidal stability of QD@$SiO_2$ under high salinity condition.

**3.3.3 Photooxidation.** The long-term photochemical stability of QDs is also a crucial issue for some applications, especially for biomedical-related studies, since the photooxidation affects the emission stability of colloidal QDs by corroding the surface of QDs. To investigate the photostability of our obtained QD@$SiO_2$, the samples of $QD_{592}$@$SiO_2$ in PBS buffer with pH 7 were irradiated by a 6-watt UV light at 254 nm at air atmosphere at room temperature. The photostability of AMP-QDs was also measured under identical conditions as a comparison. The temporal evolution of relative PL intensity of both samples was shown in Fig. 6A. It was found that after the onset of irradiation, the PL intensities of both QD@$SiO_2$ and AMP-QDs samples increased obviously, which is consistent to the reported results in the literatures.[23,56] The photo-enhancement effect was commonly attributed to the surface rearrangement of ligands and/or photocatalytic annealing of surface

atoms to repair defects and recombination centers.[66] After approaching maximum value (4h for QD@$SiO_2$, and 1 h for AMP-QDs), though the PL intensities of both samples decreased gradually, the PL intensities of QD@$SiO_2$ decreased much slower than that of AMP-QDs. Within 14 h of irradiation, the PL intensity of AMP-QDs decreased to 40% of the initial value and the aggregation of AMP-QDs was observed, while the PL intensity of QD@$SiO_2$ was almost retained (95% of the initial value) and the QD@$SiO_2$ were still homogeneously dispersible in PBS buffer. As expected, QD@$SiO_2$ exhibited superior photo-stability.

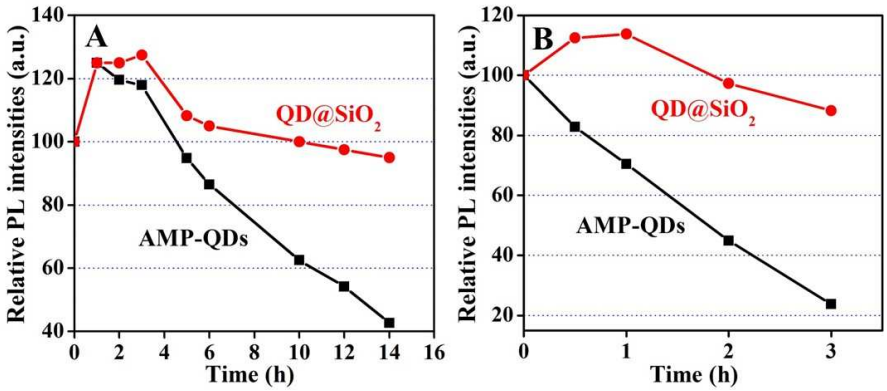


**Fig. 6** (A) Temporal evolution of PL intensities of AMP-QDs and QD@$SiO_2$ under the irradiation by a UV lamp at 254 nm excitation. (B) Temporal evolution of PL intensities of AMP-QDs and QD@$SiO_2$ in the process of heating at 100 $^oC$. The first measurement point corresponds to samples at room temperature.

**3.3.4 Thermal stability.** Temperature is another important parameter for the applications of QDs. It has been proven that coating is expected to reduce surface degradation of QDs (such as oxidation) association with the enhancement of thermal stability.[67] To investigate the thermal stability, both $QD_{592}$@$SiO_2$ and AMP-QDs in PBS buffer (pH=7) was evaluated by monitoring the evolution of relative luminescence intensity at 100 $^oC$ in nitrogen atmosphere. To investigate the thermal stability, the purified QD@$SiO_2$ and AMP-QDs samples were loaded in a closed container and immersed in a water-bath with temperature of 100 $^oC$. As shown in Fig. 6B, the PL QYs of QD@$SiO_2$ have a 10–20% increase after heating 1 h and then decreased gently, possibly because of the perfected wrap of the surface ligand around the QDs induced by the heating effect.[68] The PL intensity retained *ca.* 98 and 86% of the initial value at room temperature with heating time of 2 h, and 3 h, respectively. Furthermore, the

$QD@SiO_2$ could still keep homogenously dispersible at solution with the heating time up to 3 h. In comparison, the PL intensity of AMP-QDs decreased much more sharply. With heating time up to 3 h, the PL intensity dropped to 22% of the initial value and aggregation of QDs occurred. It demonstrates that our obtained $QD@SiO_2$ exhibited excellent thermal stability in boiling water, much better than that of AMP-QDs.

### 3.4 Cytotoxicity assay

The cytotoxicity of $QD@SiO_2$ in Hela cells by using a MTT cell viability assay has been investigated. Fig. 7 shows the viability of the cells labeled with six different concentrations of uncoated and silica coated AMP-QDs, ranging from 0 nM to 600 nM. The cell viability of blank control (i.e. untreated cells) was set as "100%", and the absorbance value of each sample was compared to that of the blank control. For $QD@SiO_2$, the cell viability almost kept 100% even at 600 nM concentration after 24 h incubation, which could be attributed to the good protection against core QDs dissolution from the effective shell passivation. In comparison, cell viability was reduced to *ca*. 50% after exposure to 600 nM of AMP-QDs for 24 h. Thus, AMP-QDs without a silica shell showed the cytotoxicity, which may be induced by the release of highly toxic Cd ions. These results demonstrate that a silica shell can efficiently diminish the influence of heavy metal ions to the biological system.

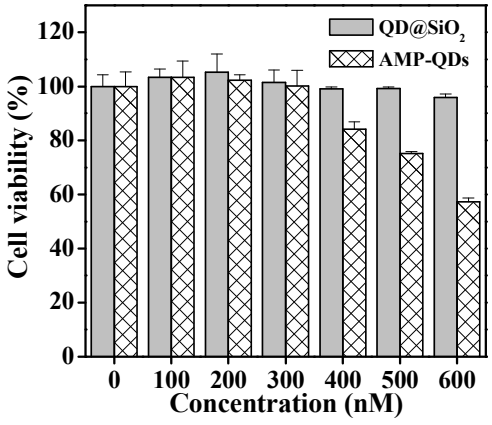


**Fig. 7** Cytotoxicity assay performed on HeLa cells incubated for 24 h with AMP-QDs and $QD@SiO_2$ at different concentrations.

### 3.5 In *vitro* cell bioimaging

In this research, we examined the cellular uptake $QD_{592}@SiO_2$ conjugated with folic acid in DMEM cell culture medium to explore their targeting capability in intracellular imaging. The surface of $QD@SiO_2$ was first functionalized with amino groups by surface-grafting of APTES. The successful grafting of amino-containing APTES to $QD@SiO_2$ was proved by fluorescamine experiment as shown in Fig. S2. Then, as-prepared amino-functionalized $QD@SiO_2$ was conjugated with FA by DCC chemical strategy, followed by the incubation with FA receptor-positive Hela cells and receptor-negative A549 cells for 1 h, respectively. Fig. 8 displays the confocal fluorescence images of the uptake of the $QD@SiO_2$-FA, and each row of panels shows representative bright field images (left), 600-nm emitting $QD@SiO_2$-FA (red), DAPI (blue), and the merged fluorescent composite images (right). As expected, the uptake of the $QD@SiO_2$-FA by Hela cells is very high. As can be seen from Fig. 8B, the pronounced fluorescence intensity of $QD@SiO_2$-FA in the Hela cells was detected, demonstrating that the substantial intracellular uptake of $QD@SiO_2$-FA took place after incubation with receptor-positive Hela cells for 1 h. On the contrary, almost no fluorescence was detectable in receptor-negative A549 cells when $QD@SiO_2$-FA was incubated with A549 cells for 1 h (Fig. 8A). To support the receptor-mediated endocytosis of the nanocomposites, we also conducted comparison experiments through the incubation of receptor-positive Hela cells with free $QD@SiO_2$ under the same experimental conditions. As a result, almost no luminescence was observed, as shown in Fig. 8C. These results show that specific binding takes place between $QD@SiO_2$-FA and receptor-positive Hela cells through the folic acid, indicating the potential of $QD@SiO_2$-FA as robust biomarkers.

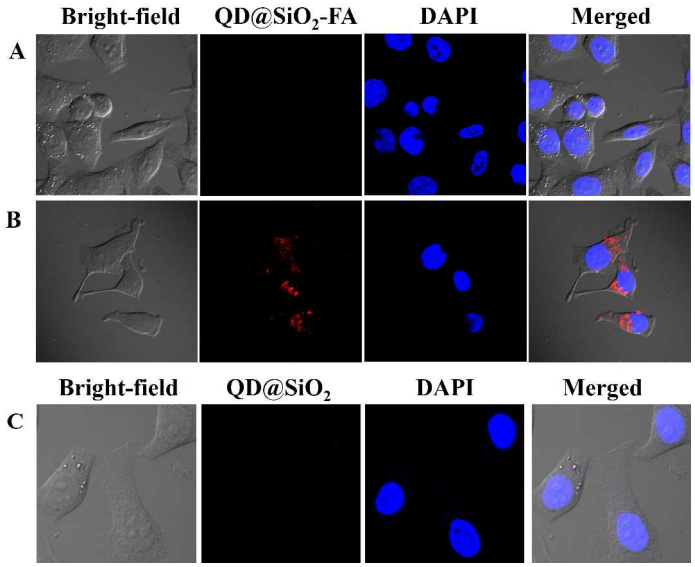


**Fig. 8** Images of (A) A549 cells (FA receptor-negative) cells and (B) Hela (FA receptor-positive) cells incubated with QD@$SiO_2$-FA for 1 h. (C) Hela cells incubated with plain QD@$SiO_2$ for 1 h. Each row shows representative bright field images (left), QD emission (red), DAPI (blue), and the merged fluorescent composite images (right).

## 4. Conclusions

In summary, owing to the super dispersibility in alcohol/water media and high luminescence efficiency of AMP-QDs, we have successfully prepared high-quality QD@$SiO_2$ *via* the typical Stöber method. The obtained QD@$SiO_2$ retained the high PL brightness of the initial oil-soluble QDs along with tunable small size (less than 30 nm) by simple variation of TEOS amount used. It should be noted that the morphology and size distribution of the resultant QD@$SiO_2$ was rather uniform, and one QD was encapsulated in each silica sphere to give monodispersed QD in silica shell in most cases. Moreover, QD@$SiO_2$ exhibited extraordinary photo and colloidal stability over extended periods of time in a broad pH range (3–13), high salt concentrations (up to 4M NaCl solution), and thermal treatment at 100 $^{o}$C. By using a MTT cell viability assay, the silica shell of QD@$SiO_2$ was proved to diminish the cytotoxicity of QD in the cell lines. Furthermore, the functionalized QD@$SiO_2$ conjugated with FA exhibited excellent targeting capability toward receptor-positive Hela cells over receptor-negative A549 cells in intracellular imaging. These features demonstrate that the QD@$SiO_2$ could be served as a versatile luminescent probe in various bioapplications.

## Acknowledgements

We thank the National Natural Science Foundation of China (No. 21175043 and 21301059), Chenguang Program of the Shanghai Education Commission (11CG31), the Science and Technology Commission of Shanghai Municipality (11JC1403100, 12NM0504101), and the Fundamental Research Funds for the Central Universities.

## Notes and references

*Shanghai Key Laboratory of Functional Materials Chemistry, Institute of Applied Chemistry, East China University of Science and Technology, Shanghai 200237, China.*

*Email: zhongxh@ecust.edu.cn; Fax: +86 21 6425 0281*

† Electronic Supplementary Information (ESI) available: The procedure of synthesis of CdSe/CdS/ZnS core/shell/shell QDs, The PL spectra of $QD_{592}$ and corresponding QD@$SiO_2$ with the amounts of 10 μL and 20 μL of TEOS, PL emission ($\lambda_{ex}$ = 390 nm) spectra of QD@$SiO_2$ and APTES grafting QD@$SiO_2$ with addition of fluorescamine. See DOI: 10.1039/c000000x/

1 D. V. Talapin, J. S. Lee, M. V. Kovalenko and E. V. Shevchenko, *Chem. Rev*., 2010, **110**, 389.

2 J. Wang, I. Mora-Sero, Z. X. Pan, K. Zhao, H. Zhang, Y. Y. Feng, G. Yang, X. H. Zhong and J. Bisquert, *J. Am. Chem., Soc*. 2013, **135**, 15913.

3 S. V. Kershaw, A. S. Susha and A. L. Rogach, *Chem. Soc. Rev.* 2013, **42**, 3033.

4 J. B. Wu, J. L. Zhang, Z. M. Peng, S. C. Yang, F. T. Wagner and H. Yang, *J. Am. Chem.*

*Soc.,* 2010, **132**, 4984.

5 L. J. Zhao, L. F. Hu and X. S. Fang, *Adv. Funct. Mater*., 2012, **22**, 1551.

6 P. Zrazhevskiy, M. Sena and X. H. Gao, *Chem. Soc. Rev.,* 2010, **39**, 4326.

7 J. B. Delehanty, C. E. Bradburne, K. Susumu, K. Boeneman, B. C. Mei, D. Farrell, J. B. Blanco-Canosa, P. E. Dawson, H. Mattoussi and I. L. Medintz, *J. Am. Chem. Soc.,* 2011, **133**, 10482.

8 M. Bruchez, M. Moronne, P. Gin, S. Weiss and A. P. Alivisatos, *Science,* 1998, **281**, 2013.

9 W. C. W. Chan and S. M. Nie, *Science,* 1998, **281**, 2016.

10 L. Chen, J. Wang, W. Li and H. Han, *Chem. Commun.,* 2012, **48**, 4971.

11 D. W. Deng, Y. Q. Chen, J. Cao, J. M. Tian, Z. Y. Qian, S. Achilefu and Y. Q. Gu, *Chem. Mater.,* 2012, **24**, 3029.

12 A. Gatam and F. C. J. M. van Veggle, *J. Mater. Chem. B*, 2013, **1**, 5186.

13 C. B. Murray, D. J. Norris and M. G. Bawendi, *J. Am. Chem. Soc.,* 1993, **115**, 8706.

14 Z. A. Peng and X. G. Peng, *J. Am. Chem. Soc.,* 2001, **123**, 183.

15 M. D. Regulacio and M. Y. Han, *Acc. Chem. Res*., 2010, **43,** 621.

16 C. D. Donega, *Chem. Soc. Rev.,* 2011, **40**, 1512.

17 W. Zhang, H. Zhang, Y. Feng and X. Zhong, *ACS Nano,* 2012, **6**, 11066.

18 H. Sun, F. Fang, H. Wei and B. Yang, *J. Mater. Chem. B*, 2013, **1**, 6485.

19 J. A. Kim, A. Aberg, A. Salvati and A. Dawson, *Nat. Nanotechol*., 2012, **7**, 62.

20 Y. Liu, P. Wang, Y. Wang, Z. Zhu, F. Lao, X. Liu, W. Cong, C. Chen, Y. Gao and Y. Liu, *Small,* 2013, **9**, 2440.

21 N. Zhan, G. Palui, X. Ji, M. Safa and H. Mattoussi, *J. Am. Chem. Soc.,* 2013, **135**, 13786.

22 H. Jin, J. Nam, J. Park, S. Jung, K. Im, J. Hur, J. J. Park, J. M. Kim and S. Kim, *Chem. Commun.,* 2011, **47**, 1758.

23 L. Liu, X. H. Guo, Y. Li and X. H. Zhong, *Inorg. Chem.,* 2010, **49**, 3768.

24 M. V. Kovalenko, B. Spokoyny, J. S. Lee, M. Scheele, A. Weber, S. Perera, D. Landry and D. V. Talapin, *J. Am. Chem. Soc.,* 2010, **132**, 6686.

25 N. Tomczak, R. Liu and J. G. Vancso, *Nanoscale,* 2013, **5**, 12018.

26 A. Quarta, A.Curcio, H. Kakwere and T. Pellegrino, *Nanoscale,* 2012, **4***,* 3319.

27 Y. Z. Wu, S. Chakrabortty, A. R. Gropeanu, J. Wilhelmi, Y. Xu, K. S. Er, S. L. Kuan, K. Koynov, Y. Chan and T. Weil, *J. Am. Chem. Soc.,* 2010, **132**, 5012.

28 Y. Zhang, M. Wang, Y. Zheng, H. Tan, B. Y. Hsu, Z. Yang, S. Y. Wong, A. Y. Chang, M. Choolani, X. Li and J. Wang, *Chem. Mater*., 2013, **25**, 2976.

29 D. Gerion, F. Pinaud, S. C. Williams, W. J. Parak, D. Zanchet, S. Weiss and A. P. Alivisatos, *J. Phys. Chem. B,* 2001, **105**, 8861.

30 D. K. Yi, S. T. Selvan, S. S. Lee, G. C. Papaefthymiou, D. Kundaliya and J. Y. Ying, *J. Am. Chem. Soc.,* 2005**, 127***,* 4990.

31 A. Guerrero-Martinez, J. Perez-Juste and L. M. Liz-Marzan, *Adv. Mater.,* 2010, **22***,* 1182.

32 Y. Zhu, Z. Li, M. Chen, H. M. Cooper and Z. P. Xu, *J. Mater. Chem. B*, 2013, **1**, 2315.

33 Z. Lin, X. Fei, Q. Ma, X. Gao and X. Su, *New J. Chem*., 2014, **38**, 90.

34 S. H. Liu and M. Y. Han, *Adv. Funct. Mater.,* 2005, **15***,* 961.

35 S. H. Liu and M. Y. Han, *Chem. Asian J.,* 2010, **5**, 36.

36 N. Erathodiyil and J. Y. Ying, *Acc. Chem. Res.,* 2011, **44**, 925.

37 Y. X. Liu, P. Wang, Y. Wang, Z. N. Zhu, F. Lao, X. F. Liu, W. S. Cong, C. Y. Chen, Y. Gao and Y. Liu, *Small,* 2013, **9**, 2440.

38 K. M. Wang, X. X. He, X. H. Yang and H. Shi, *Acc. Chem. Res.,* 2013, **46***,* 1367.

39 Y. H. Yang and M. Y. Gao, *Chem. Mater.,* 2007*,* **19***,* 4123.

40 S. T. Selvan, T. T. Tan and J. Y. Ying, *Adv. Mater.,* 2005*,* **17***,* 1620.

41 Z. Zhelev, H. Ohba and R. Bakalova, *J. Am. Chem. Soc.,* 2006, **128**, 6324.

42 R. Koole, M. M. van Schooneveld, J. Hilhorst, C. d. M. Donega, D. C. t Hart, A. van Blaaderen, D. Vanmaekelbergh and A. Meijerink, *Chem. Mater.,* 2008*,* **20***,* 2503.

43 L. H. Jing, C. H. Yang, R. R. Qiao, M. Niu, M. H. Du, D. Y. Wang and M. Y. Gao, *Chem. Mater*., 2010, **22**, 420.

44 Y. Zhu and Z. P. Xu, *Chem. Mater*., 2012, **24**, 421.

45 P. Yang, M. Ando and N. Murase, *Langmuir,* 2011, **27***,* 9535.

46 M. Darbandi, R. Thomann and T. Nann, *Chem. Mater.,* 2005*,* **17***,* 5720.

47 T. V. Duncan, M. A. M. Polanco, Y. Kim and S. Park, *J. Phys. Chem. C.,* 2009*,* **113***,* 7561.

48 Y. H. Yang and M. Y. Gao, *Adv. Mater.,* 2005*,* **17***,* 2354.

49 W. Stöber, A. Fink and E. Bohn, *J. Colloid Interface Sci*., 1968, **26**, 62.

50 T. Nann and P. Mulvaney, *Angew. Chem. Int. Ed.,* 2004*,* **43***,* 5393.

51 Y. Chan, J. P. Zimmer, M. Stroh, J. S. Steckel, R. K. Jain and M. G. Bawendi, *Adv. Mater.*, 2004, **16**, 2092.

52 A. L. Rogach, D. Nagesha, J. W. Ostrander, M. Giersig and N. A. Kotov, *Chem. Mater.,* 2000*,* **12***,* 2676.

53 N. R. Jana, C. Earhart and J. Y. Ying, *Chem. Mater*., 2007, **19**, 5074.

54 P. Yang, M. Ando, T. Taguchi and N. Murase, *J. Phys. Chem. C,* 2010, **114**, 20962.

55 P. Yang and N. Murase, *Adv. Funct. Mater.,* 2010, **20**, 1258.

56 L. Liu and X. H. Zhong, *Chem. Commun*., 2012, **48,** 5718.

57 L. Qu and X. Peng, *J. Am. Chem. Soc*., 2002, **124**, 2049.

58 J. J. Li, Y. A. Wang, W. Guo, J. C. Keay, T. D. Mishima, M. B. Johnson and X. Peng, *J. Am. Chem. Soc*., 2003, **125**, 12567.

59 R. Xie, U. Kolb, J. Li, T. Basche and A. Mews, *J. Am. Chem. Soc.,* 2005, **127**, 7480.

60 L. Zhou, C. Gao, X. Z. Hu and W. J. Xu, *Chem. Mater.,* 2011, **23**, 1461.

61 L. Zhou, C. Gao and W. J. Xu, *J. Mater. Chem.,* 2009, **19**, 5655.

62 H. Yang, Y. Zhuang, H. Hu, X. Du, C. Zhang, X. Shi, H. Wu and S. Yang, *Adv. Funct. Mater.,* 2010*,* **20***,* 1733.

63 M. Colilla, I. Izquierdo-Barba, S. Sánchez-Salcedo, J. L. G. Fierro, J. L. Hueso and M. Vallet-Regí, *Chem. Mater.,* 2010*,* **22***,* 6459.

64 Y. J. Wong, L. F. Zhu, W. S. Teo, Y. W. Tan, Y. H. Yang, C. Wang and H. Y. Chen, *J. Am. Chem. Soc.,* 2011*,* **133***,* 11422.

65 X. G. Hu and X. H. Gao, *ACS Nano,* 2010*,* **4***,* 6080.

66 L. Zou, Z. Fang, Z. Y. Gu and X. H. Zhong, *J. Lumin.,* 2009, **129**, 536.

67 Y. Zhang and Y. D. Li, *J. Phys. Chem. B*, 2004, **108**, 17805.

68 Y. Cui, X. Q. Gong, S. J. Zhu, Y. H. Li, W. Y. Su, Q. H. Yang and J. Chang, *J. Mater. Chem.,* 2012, **22**, 462.

**The table of contents.**

# Highly Bright Water-Soluble Silica Coated Quantum Dots with Excellent Stability

**Yunfei Ma, Yan Li, Shijian Ma, and Xinhua Zhong***

A facile Stöber method for the synthesis of isolated silica coated QDs with high PL efficiencies, tunable small size and excellent stability leads to the practical bioapplication as robust biomarkers.